CHARACTERIZATION OF PORE STRUCTURE OF ELECTRODES OF SOLID OXIDE FUEL CELLS

Akshaya Jena and Krishna Gupta
Porous Materials, Inc.
20 Dutch Mill Road
Ithaca, NY 14850

ABSTRACT

In this paper, the pore structure characteristics of two considerably different ceramic electrode materials were successfully investigated using flow porometry. Through pore throat diameters, distribution of flow rate over pore diameters and gas permeability were measured. Pore volumes measured with mercury intrusion porosimetry showed that the through pores and the blind pores were associated with considerable volume of wide parts. The results were consistent with scanning electron micrographs.

INTRODUCTION

Electrodes tend to be porous in order to permit flow of reactants, facilitate electrode reactions and permit flow of products. The important pore structure characteristics of electrodes include through pore diameters, through pore size distribution, through pore surface area, and gas permeability. Control of such pore structure characteristics is possible through process control parameters such as characteristics of starting material, forming methods, sintering temperature and sintering time. Therefore, it is important to be able to accurately measure the pore structure characteristics of electrodes of solid oxide fuel cells.

CHARACTERIZATION TECHNIQUE

Flow Porometry

For capillary flow porometry, pores of the sample are spontaneously filled with a wetting liquid and pressure of a non-reacting gas is increased on the sample to empty the pores and permit gas flow. Differential gas pressure needed for displacement of the wetting liquid in a pore is related to pore size[1].

$$p = 4 \gamma \cos \theta / D \qquad (1)$$

where p is the differential gas pressure across the pore, γ is the surface tension of the wetting liquid, θ is the contact angle of the wetting liquid, and D is the pore diameter. For pores of irregular cross-section, pore diameter, D, is defined by Equation 2.

$$[(\text{Perimeter}) / (\text{Area})]_{\text{pore}} = [(\text{Perimeter}) / (\text{Area})]_{\text{circular opening of diameter, D}} = 4 / D \qquad (2)$$

Differential gas pressure and flow rates through a dry sample and the same sample with its pores filled with a wetting liquid are measured. Various pore structure characteristics

including largest through pore throat diameter, mean through pore throat diameter, pore distribution, and gas permeability are computed from measured values.

The instrument used in this investigation is shown in Figure 1. The instrument was fully automated in order to obtain accurate data. Test execution, data acquisition, data storage and data reduction were conveniently carried out using Windows based soft ware. The instrument accurately measured flow rates and pore sizes over a wide range. The special design of the instrument permitted measurement of very small flow rates through some of the dense electrodes. It was possible to test samples having a variety of shapes and sizes.

Figure 1. The Microflow Porometer used in this investigation

Mercury Intrusion Porosimetry

A nonwetting liquid like mercury cannot enter pores spontaneously. Increase of pressure on mercury forces mercury into pores. The pressure is related to pore diameter[2].

$$D = - 4 \gamma \cos \theta / p \qquad (3)$$

where D is pore the diameter defined by Equation 2, γ is the surface tension of the nonwetting liquid mercury, θ is the contact angle of mercury, and p is the intrusion pressure. Intrusion volume and intrusion pressure are measured. Intrusion pressure gives diameter and intrusion volume gives pore volume of through and blind pores.

The mercury intrusion porosimeter used in this investigation is shown in Figure 2. The special design of the instrument prevented exposure to mercury. The test execution, data acquisition and data reduction were fully automated for accurate data.

Materials

Samples of materials for several components of SOFC were investigated. One was NiO-YSZ. The other was a two-phase composite of two oxides. The composites I and II contained different percentages of nickel oxide.

RESULTS AND DISCUSSIONS

Through Pore Throat Diameters

Capillary Flow Porometry detects the presence of a pore when the wetting liquid is completely removed from the pore and gas starts flowing through the pore. The differential

pressure at which a pore becomes completely empty is the pressure required to displace the wetting liquid from the pore throat because this is the maximum pressure needed to remove liquid from the pore (Equation 1). Therefore, the pore diameter computed from the differential pressure at which gas flow starts through a pore is the pore throat diameter (Figure 3).

Figure 2. The Mercury Intrusion Porosimeter used in this investigation

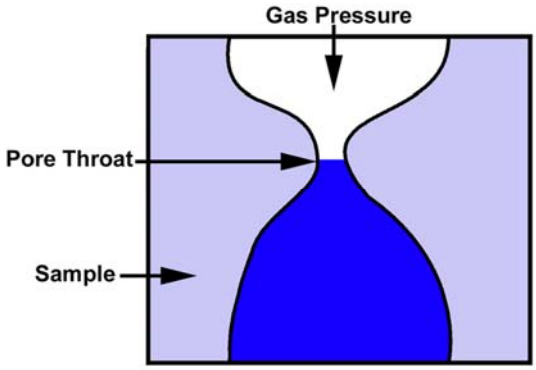

Figure 3. Pore diameters measured by flow porometry

In order to measure the through pore throat diameters, the ceramic components were tested by flow porometry. Such components are likely to contain blind pores. Therefore, the samples were evacuated, completely wetted with the wetting liquid galwick having a surface tension of 16 dynes/cm and tested in microflow porometer capable of measuring very low flow rates. The flow rates through wet and dry samples as functions of differential pressure are shown in Figure 4.

The pore throat diameters are computed from the measured differential pressure. The largest through pore throat diameter is computed from pressure to initiate flow through wet sample. The mean flow through pore throat diameter is obtained from the mean flow pressure. The mean flow pressure is the pressure at which the flow through the wet sample becomes equal to the half-dry flow (Figure 4). The half-dry flow is half of the flow through the dry sample at any pressure. The range of measured through pore throat diameters of two materials designed for SOFC are listed in Table I.

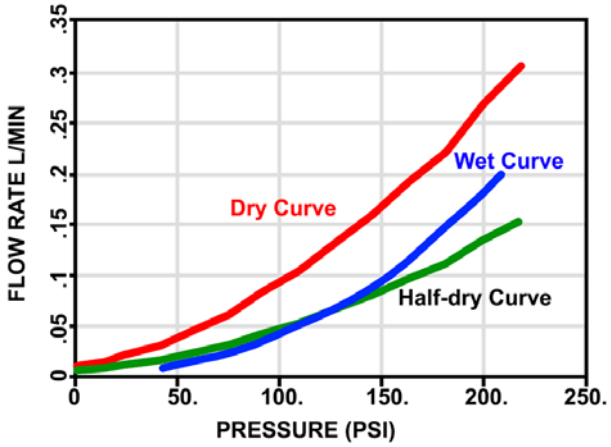

Figure 4. Variation of air flow rate with the differential pressure through YSZ (PSI =6.895 kPa)

Table I. Throat diameters of through pores

	The largest pore, μm	The mean flow pore, μm
YSZ	0.151	0.053
Composite I	487	237

Flow Distribution Over Through Pore Throat Diameters

Flow distribution over through pore throat diameters is determined by the number of different diameter pores. Flow distribution is given by distribution function**,** f:

$$f = - d[(F_w/ F_d)\times 100] / dD \qquad (4)$$

where F_w and F_d are flow through wet and dry samples respectively. The flow distribution in the composite II is shown in Figure 5. The distribution function in this figure is normalized taking the maximum value of the function to be 100. The area under the function in any pore diameter range is proportional to the percentage of flow in that diameter range. Pores with appreciable contribution to flow are listed in Table II. The distribution function can also yield the fractional pore number distribution.

Table II. Pores with appreciable contributions to flow

Material	Distribution	Diameter range, μm
YSZ	Narrow, Bimodal	0.04 – 0.08
Composite I	Broad, Unimodal	50 – 250

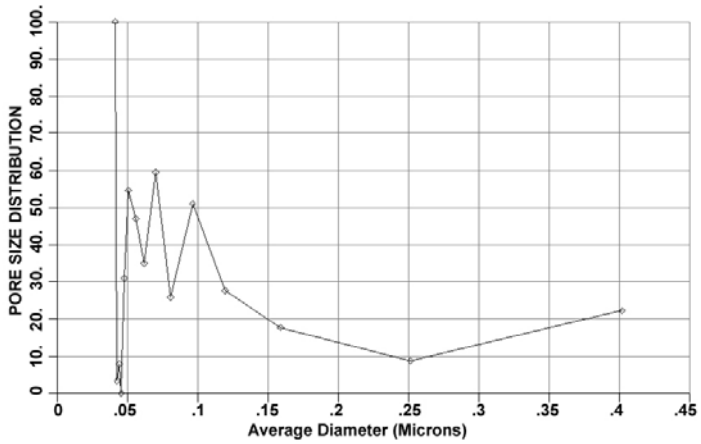

Figure 5. Flow distribution over through pore throat diameters in composite II

The pore structures of the ceramic electrode materials may be noted from their Scanning Electron Micrographs (Figure 6). The measured pore diameters are consistent with the micrographs. Pores in YSZ are much smaller than those in the composite.

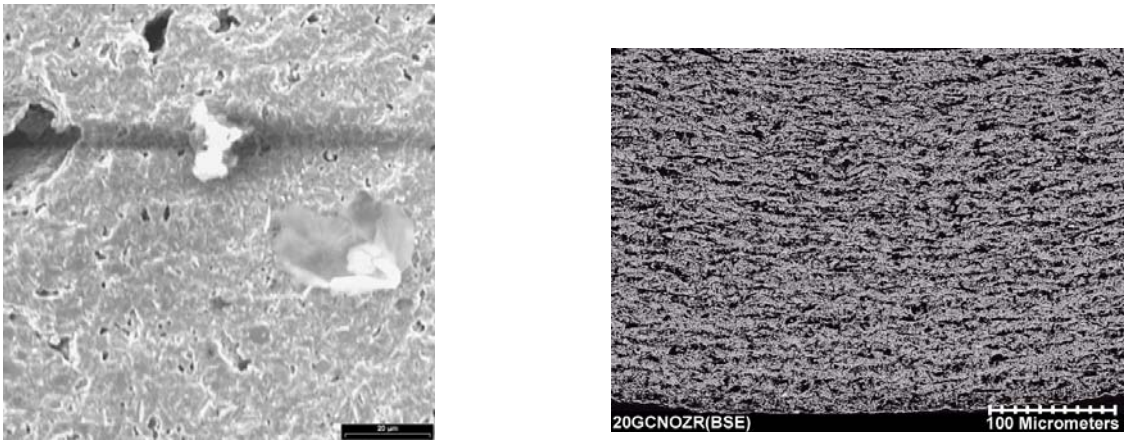

(a) (b)

Figure 6. SEM micrographs of ceramic electrode materials, (a) YSZ and (b) Composite

All Diameters of Through and Blind Pores

Each pore normally has many pore diameters. All diameters of through and blind pores are measured by intrusion porosimetry (Figure 7). The measured pore diameters are shown in Figure 8.

Volume of Through and Blind Pores

As illustrated in Figure 7 volumes of through and blind pores are measurable by mercury intrusion porosimetry. The results of YSZ are illustrated in Figure 8.

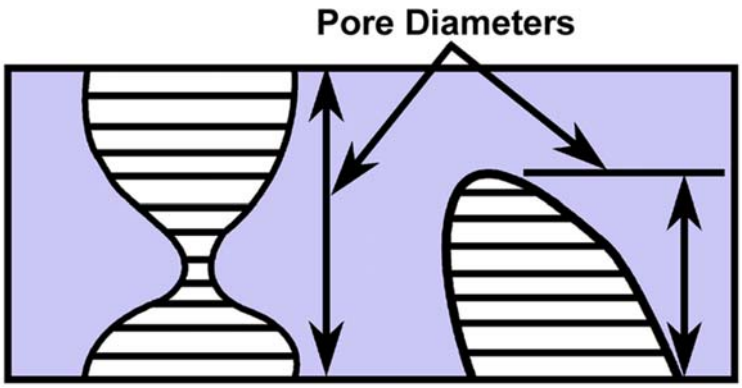

Figure 7. Diameters and volumes of through and blind pores measured by intrusion porosimetry

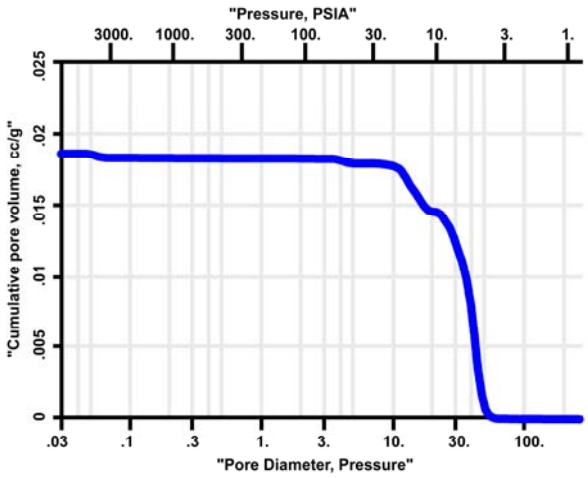

Figure 8. All diameters of pores and volumes of through and blind pores in YSZ

Distribution of Pore Volume Over Through and Blind Pore Diameter

Volume distribution over pore diameters is given in terms of the distribution function, fv;

$$fv = - (dV/d \log D) \quad (5)$$

where V is the pore volume. Distribution of through and blind pore volume over their diameters in YSZ is shown in Figure 9. The area under the function in any pore size range gives volume of pore in that range. Several pore peaks can be seen in the distribution curve.

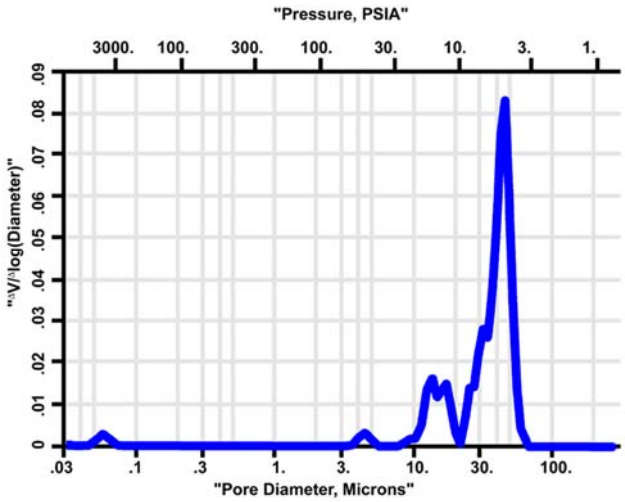

Figure 9. Distribution of volume of through and blind pores over their diameters in YSZ

Shape of Through Pores

Contributions to pore volumes by pores of different sizes obtained from the pore peaks of YSZ are listed in Table III. The through pores in YSZ have throat diameters close to 0.05 μm and have very small pore volumes associated with pore throats. This result is consistent with the small gas flow rates (0.05 l/min) through YSZ (Figure 4). The measured large pore diameters and large volumes must be associated with the wide mouths of through pores and blind pores. The presence of such pores in YSZ is seen in the SEM in Figure 6.

Table III. Contributions to pore volumes by pores of different sizes

Pore diameter	Pore volume
~ 40 μm	79 % Pore Volume
~ 15 μm	17 % Pore Volume
~ 4.5 μm	2.5 % Pore Volume
~ 0.06 μm	1.5 % Pore Volume

Permeability

Gas permeability was calculated from gas flow rate through dry sample using Darcy's law.

$$\underline{F} = - [k A / \mu] (dp /dx) \qquad (6)$$

where k is permeability, $\underline{F}$ is flow rate in volume at average pressure and test temperature, A is area of the sample, μ is viscosity of fluid, and (dp/dx) is pressure gradient across the sample. Flow rates are measured in terms of flow, F, at standard temperature and pressure. Expressing $\underline{F}$ in terms of F and integrating over the thickness of the sample;

$$F = k [(A T_{s)} / (2 \mu l p_s T)] [pi^2 - p_0^2] \qquad (7)$$

where T_s is standard temperature, l is thickness of sample, p_s is standard pressure, T is experimental temperature, p_i is inlet pressure, and p_0 is outlet pressure. Gas flow rates measured through the composite II as functions of differential is shown in Figure 10. The calculated air permeability of the composite is 9.96×10^{-3} Darcies. Permeability could also be expressed in any other unit including Frazier, Gurley and Rayle.

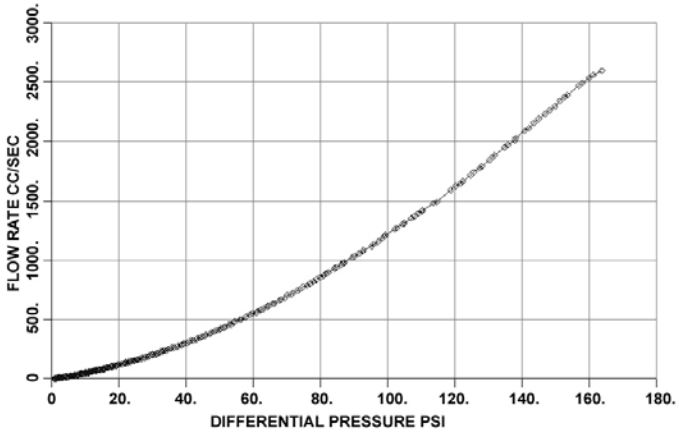

Figure 10. Variation of airflow rate through the composite II as a function of pressure

SUMMARY AND CONCLUSION

The pore structure characteristics of two materials developed for SOFC, were investigated by capillary flow porometry. The pore structure characteristics, through pore throat diameters, the largest through pore throat diameter, mean flow through pore throat diameter, flow distribution over pore diameter, pores exhibiting appreciable flow, and gas permeability were successfully measured.

YSZ exhibited very low flow, a bimodal distribution, the largest through pore throat diameter of 0.151 μm, mean flow through pore throat diameter of 0.053 μm, and pore diameters of 0.04–0.08 μm exhibiting appreciable flow. Composite I exhibited a broad unimodal distribution, the largest through pore throat diameter of 487 μm, mean flow through pore throat diameter of 237 μm, and pore diameters of 50-250 μm exhibiting appreciable flow. In composite II, the distribution peak was observed at 0.05-0.12 μm and the permeability was 9.96×10^{-3} Darcies.

REFERENCES

[1]Akshaya Jena and Krishna Gupta, "Liquid Extrusion Techniques for Pore Structure Evaluation of Nonwovens," *International Nonwovens Journal*, Fall, 45-53 (2003).

[2]Akshaya Jena and Krishna Gupta, "Characterization of Pore Structure of Filtration Media," *Fluid particle Separation Journal*, **14**, 227-241 (2002).